Experimental Liver Cirrhosis Induced by Alcohol and Iron

Hidekazu Tsukamoto, Walter Horne, Seiichiro Kamimura, Onni Niemelä, Seppo Parkkila, Seppo Ylä-Herttuala, and Gary M. Brittenham

Departments of Medicine and Nutrition, Case Western Reserve University at MetroHealth Medical Center and Department of Veterans Affairs Medical Centers, Cleveland, Ohio 44109; and Department of Clinical Chemistry, University of Helsinki, and AIV Institute, University of Kuopio, Finland

Abstract

To determine if alcoholic liver fibrogenesis is exacerbated by dietary iron supplementation, carbonyl iron (0.25% wt/vol) was intragastrically infused with or without ethanol to rats for 16 wk. Carbonyl iron had no effect on blood alcohol concentration, hepatic biochemical measurements, or liver histology in control animals. In both ethanol-fed and control rats, the supplementation produced a two- to threefold increase in the mean hepatic non-heme iron concentration but it remained within or near the range found in normal human subjects. As previously shown, the concentrations of liver malondialdehyde (MDA),[1] liver 4-hydroxynonenal (4HNE), and serum aminotransferases (ALT, AST) were significantly elevated by ethanol infusion alone. The addition of iron supplementation to ethanol resulted in a further twofold increment in mean MDA, 4HNE, ALT, and AST. On histological examination, focal fibrosis was found < 30% of the rats fed ethanol alone. In animals given both ethanol and iron, fibrosis was present in all, with a diffuse central–central bridging pattern in 60%, and two animals (17%) developed micronodular cirrhosis. The iron-potentiated alcoholic liver fibrogenesis was closely associated with intense and diffuse immunostaining for MDA and 4HNE adduct epitopes in the livers. Furthermore, in these animals, accentuated increases in procollagen α1(I) and TGFβ1 mRNA levels were found in both liver tissues and freshly isolated hepatic stellate cells, perisinusoidal cells believed to be a major source of extracellular matrices in liver fibrosis. The dietary iron supplementation to intragastric ethanol infusion exacerbates hepatocyte damage, promotes liver fibrogenesis, and produces evident cirrhosis in some animals. These results provide evidence for a critical role of iron and iron-catalyzed oxidant stress in progression of alcoholic liver disease. (*J. Clin. Invest.* 1995. 96:620–630.) Key words: collagen • TGFβ1 • non-heme iron • lipid peroxidation • hepatic stellate cells

Introduction

Hepatic fibrogenesis in alcoholic liver disease is an intricate process, which appears to involve a metabolic product of ethanol oxidation (1, 2), cytochrome P450 induction (3, 4), enhanced oxidative stress (5, 6), depletion of antioxidant defenses (7), lipid peroxidation (8), generation of aldehydic products (8), the effects of mitogenic and fibrogenic cytokines (9, 10), and complex interactions between liver parenchymal and nonparenchymal cells (9, 10), with the hepatic stellate cells (Ito cells, hepatic lipocyte or fat-storing cell) now recognized as the primary source of extracellular matrix (10). The spectrum of alcoholic liver disease is partially reproduced in a rat model of intragastric ethanol infusion (11, 12). Focal centrilobular liver necrosis is evident after 5–6 wk of feeding high fat diet (HFD) plus ethanol and liver fibrogenesis is initiated between the 9th and 16th wk. At the 16th week, the fibroproliferative activation of hepatic stellate cells is manifested by increased DNA synthesis together with enhanced gene expression of collagen and transforming growth factor-β1 (TGFβ1) (13). In this model, the severity of liver damage has been shown to depend on the magnitude of oxidative stress. For example, diets high in polyunsaturated fat and low in carbohydrate which induce cytochrome P4502E1 (CYP2E1) (14), enhance ethanol-induced oxidative stress, compromise glutathione homeostasis (7), and produce alcoholic liver necrosis, inflammation, and fibrosis (3, 15, 16). Induction of CYP2E1 in animals with alcoholic liver injury markedly increases the sensitivity of isolated hepatic microsomes to iron-catalyzed lipid peroxidation (4). Conversely, inhibition of CYP2E1 by diallyl sulfide ameliorates the early changes of alcoholic liver injury (17). Furthermore, the extent of alcoholic liver fibrosis correlates significantly with hepatic levels of products of lipid peroxidation such as malondialdehyde (MDA) and 4-hydroxynonenal (4HNE) (8), aldehydes that directly stimulate collagen synthesis and/or gene expression by fibroblasts (18) and hepatic stellate cells (19).

One limitation of the intragastric infusion model was that only early or mild fibrosis was produced; cirrhosis was not observed even with more prolonged exposure to ethanol. Measurements of the hepatic iron in the rats used in our previous study (8) indicated that the concentrations of non-heme iron present were in the lower portion of the normal range for human adults (57–681 μg Fe per gram of liver, wet weight) (20). Accordingly, we hypothesized that the addition of dietary iron supplementation to intragastric ethanol infusion would increase

This study was presented in part at the annual meetings for American Association for Studies of Liver Diseases in Chicago, IL, 1992 and 1994 and at the Digestive Disease Week in Boston, MA, 1993.

Address correspondence to Dr. H. Tsukamoto, Division of GI and Liver Diseases, Department of Medicine, University of Southern California School of Medicine, 1355 San Pablo Street, Suite 125, Los Angeles, CA 90033-4581. Phone: 213-342-5107; FAX: 213-342-5567.

Received for publication 24 July 1994 and accepted in revised form 2 March 1995.

1. *Abbreviations used in this paper:* 4HNE, 4-hydroxynonenal; CYP2E1, cytochrome P4502E1; GSSG, glutathione, oxidized; MDA, malondialdehyde.

J. Clin. Invest.

0021-9738/95/07/0620/11 $2.00
Volume 96, July 1995, 620–630

hepatic non-heme iron which might then enhance iron-catalyzed oxidant stress, increase the generation of aldehydic products of lipid peroxidation and promote hepatic fibrogenesis. The goal of dietary iron supplementation was not to produce iron overload but rather to increase the hepatic nonheme iron into the upper portion of the normal range for human adults. The addition of dietary iron supplementation to intragastric infusion of ethanol was found to increase lipid peroxidation and the formation of peroxidation-derived protein adducts, exacerbate hepatocyte damage, accelerate and potentiate fibrogenesis, and to produce micronodular hepatic cirrhosis in some animals.

Methods

Animal models. The animal protocol described in this study was approved by the Institutional Care and Use Committee of Case Western Reserve University and is in full compliance with the Public Health Service *Guide for the Care and Use of Laboratory Animals.* The rat model of alcoholic liver fibrosis has been described in detail elsewhere (11, 12). In brief, male Wistar rats weighing 325–375 grams were implanted with long-term gastrostomy catheters to enable continuous intragastric infusion of the high fat diet (25% of calories as corn oil) plus increasing concentrations of ethanol or isocaloric dextrose solution for 16 wk. Ethanol intake at the end of experiment was 49% (16g/kg per day) of total calories. Carbonyl iron was added at 0.12% (wt/vol) during the first week and at 0.25% after the second week to the diet given to the iron-supplemented alcohol-fed and pair-fed control groups. At the ninth week, animals were anesthetized with ketamine and xylazine to collect blood for determination of aminotransferase levels and to perform aseptic liver biopsy to assess the hepatic non-heme iron concentration and progression of liver pathology. At the end of the 16-wk period, all animals were killed, the whole or a portion of liver removed, weighed, cut into small portions for various biochemical, molecular biological, and histological examinations described below.

Measurements of non-heme iron, lipid peroxidation, glutathione and hydroxyproline. The non-heme iron concentrations in plasma and liver were measured by a bathophenanthroline sulfonate-thioglycolic acid chromogen assay (21). A piece of liver was quickly homogenized in 1.15% KCl containing 0.2% butylated hydroxytoluene at 4°C and used immediately for MDA and 4HNE assays. The measurement of MDA equivalents was performed according to the method described by Uchiyama and Mihara (22) using 1% phosphoric acid and 0.6% thiobarbituric acid. To determine the level of free 4HNE, the homogenate was first incubated with 0.1% 2,4-dinitrophenylhydrazine in ethanol and sulfuric acid (9:1) in the dark for 12 h to form dinitrophenylhydrazone derivatives of alkenals (8, 23, 24). These derivatives were extracted with dichloroethane and separated by thin-layer chromatography. The area corresponding to the derivative of authentic 4HNE was scraped, extracted, redissolved and injected into a HPLC reverse-phase column (Ultrasphere, 5 μm octadecyl silica gel; Alltech Associates, Inc., Deerfield, IL) to separate and quantify the 4HNE derivative (8, 23, 24). For determination of hepatic concentrations of GSH and GSSG, portions of the livers were immediately snap-frozen in liquid nitrogen and stored at −80°C until assayed by the method of Griffith (25) as modified by Allen and Arthur (26) using the glutathione reductase-5′,5′-dithiobis-(2-nitrobenzoic acid) recycling assay. To estimate the collagen content of the liver, the release of hydroxyproline in hydrolysate of the liver was determined using Ehrlich's reagent (27).

Liver histology and blood aminotransferase assays. Liver tissues were fixed in a 10% formalin solution, processed, and stained with hematoxylin and eosin, Sirius red, and reticulin stains. Using light microscopy, an observer unaware of the treatment group systematically graded sections obtained from multiple liver lobes for fatty liver, necrosis, inflammation, perivenular fibrosis, bridging fibrosis, and cirrhosis. At the time of sacrifice, three mL venous blood was collected via venipuncture of inferior vena cava and serum ethanol, ALT and AST levels were determined on a CX-7 computer-controlled biochemical analyzer (Beckman Diagnostic Instruments Inc., Brea, California) and a Kodak Ektachem 750 autoanalyzer (Eastman Kodak Co., Rochester, New York).

Immunohistochemical procedures. Serial paraffin-embedded sections were used for immunostaining for MDA- and 4HNE-adduct epitopes with the immunoperoxidase technique (28). After deparaffinization, sections were pretreated with swine serum and incubated with primary guinea pig anitsera (1:500 in 1% BSA-PBS). After washing three times in PBS, the sections were retreated with swine serum to block nonspecific binding. The secondary antibody was biotinylated anti-guinea pig antiserum (1:300 in 1% BSA-PBS). (Amersham, UK). Specific staining was detected using peroxidase-conjugated streptavidin (1:600 in PBS) (Dakopatts, Copenhagen, Denmark), and 9 mg diaminobenzidine tetrahydrochloride (DAB) in 15 mL PBS.

Preparation of antisera. Antisera against MDA-LDL were raised by immunizing male guinea pigs with homologous MDA-LDL prepared as previously described (28). The priming immunization was an intradermal injection of 150 μg of antigen in 0.5 ml of PBS and 0.5 ml of Freund's complete adjuvant. Boosters were 100 μg of antigen in Freund's incomplete adjuvant at 14-d intervals. Conjugation of 4HNE to LDL was carried out according to the procedure described earlier (29, 30). Polyvalent antisera were generated by immunizing male guinea pigs with homologous 4HNE-LDL as described for the antisera against MDA-LDL.

Isolation of hepatic stellate cells. Hepatic stellate cells were isolated from the liver by in situ liver digestion and discontinuous gradient ultracentrifugation (13). Without the prior vitamin A treatment, the livers were digested enzymatically with pronase and collagenase by in situ perfusion. For fibrotic livers, we generally increased collagenase concentration by 30–70% compared to those employed for the control livers. Parenchymal cells were removed by centrifugation of the digest at 50 *g* for 1 min, and nonparenchymal cells were recovered from the supernatant by centrifugation at 500 *g* for 7 min. The nonparenchymal cells were laid on top of the four density gradients of arabinogalactan (LARCOLL; Sigma Chemical Co., St. Louis, MO), and centrifuged at 21,400 rmp for 35 min at 25°C. A pure fraction of hepatic stellate cells was recovered from the interface between the medium and the density of 1.038. The purity of the cells was assessed by phase contrast microscopy and UV excited fluorescence microscopy, and the viability by trypan blue exclusion. The purity of the cells from rats given high fat diet, high fat diet with iron, high fat diet with ethanol, and high fat diet with iron and ethanol, averaged 97, 96, 93, and 92%, respectively, and the viability exceeded 97% in all four groups.

Northern blot analyses for collagen and TGFβ1 mRNA. A portion of the liver and all of freshly isolated hepatic stellate cells were immediately homogenized in 4 M guanidinium thiocyanate followed by phenol-chloroform extraction to isolate total RNA (31). 20 μg of RNA samples were electrophoresed on formaldehyde-containing agarose gel (1.2%) and transferred to nylon membranes (NYTRAN; Schleicher & Schuell, Keene, NH). Ethidium bromide staining was used to assess the equal loading and the intact nature of RNA samples. Northern blot hybridization was performed with cDNA for rat procollagen α1(I) and human TGFβ1 (32, 33), which were labeled by ^{32}P-dCTP using the random method. An β actin cDNA was used as an internal control. The filters were prehybridized and hybridized at 50°C in 10× Denhardt's solution, 0.5% SDS, 50 μM Tris, 5 μM EDTA, 5× standard saline citrate (SSC), 150 μg/ml sonicated salmon sperm DNA, and 10% dextran sulfate. The filters were washed twice at room temperature in 2× SSC and 0.1% SDS, twice at 50°C in 2× SSC and 1% SDS, and twice at 50°C in 0.1× SSC and 0.1% SDS with each washing period lasting 30 min. Autoradiography was performed with Kodak XAR films and intensifying screens at −80°C. Bands corresponding to transcripts were scanned in a densitometer to express steady state levels with densitometric units which were subsequently normalized to that of β actin. The normalized values were then compared to those of pair-fed controls to assess relative changes.

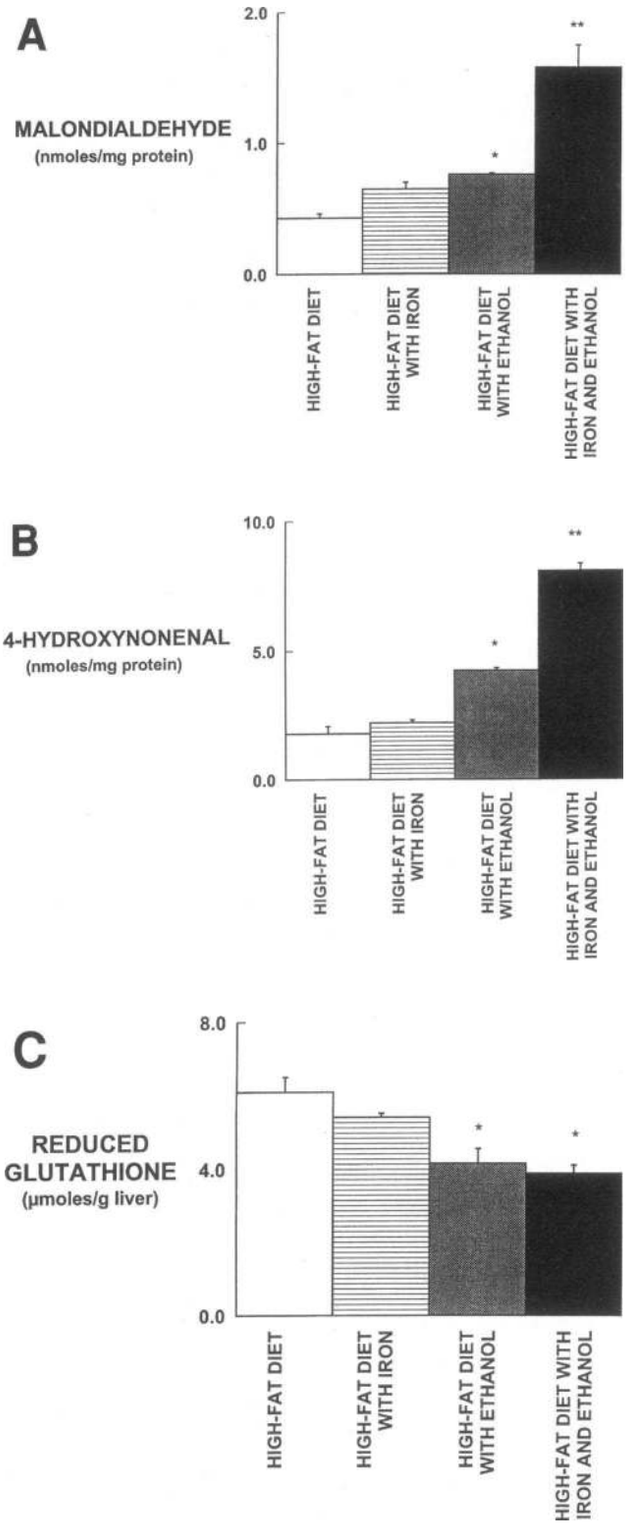

Figure 1. MDA, 4HNE, and GSH levels. The liver concentrations of MDA (*A*), 4HNE (*B*), and GSH (*C*) were determined as described in Methods, in rats fed high fat diet (n = 7), high fat diet with iron (n = 8), high fat diet with ethanol (n = 5), or high fat diet with iron and ethanol (n = 8) for 16 wk. Note prominent increases in MDA and 4HNE levels in the group given high fat diet with iron and ethanol as compared to moderate increases in these aldehydes in the group of high fat diet with ethanol. Hepatic GSH levels were similarly depressed in both high fat diet with ethanol and high fat diet with iron and ethanol groups as compared to the respective controls.* $P < 0.01$ compared to the corresponding controls; ** $P < 0.01$ compared to the high fat diet with ethanol.

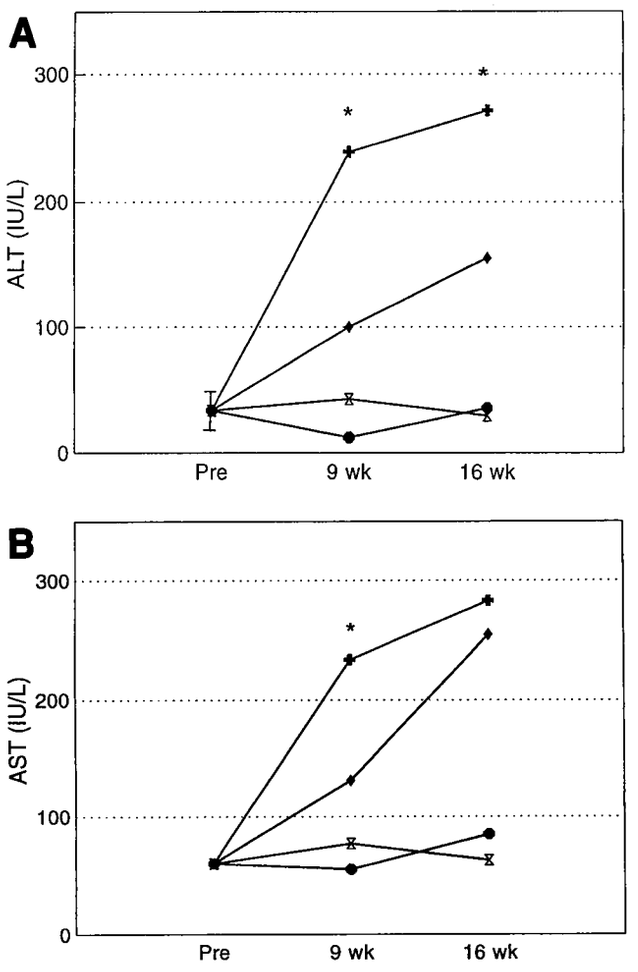

Figure 2. Plasma ALT (*A*) and AST (*B*) concentrations. Venous blood samples were collected before (Pre) and 9 wk (9 wk) and 16 wk (16 wk) after the commencement of respective dietary regimens for determination of plasma ALT and AST levels. Note accentuated increases in both ALT and AST levels in the group given high fat diet with iron and ethanol (-✦-, n = 8) as compared to the group of high fat diet with ethanol (-◆-, n = 5). Both control groups: high fat diet (-●-, n = 7) and high fat diet with iron (-⧖-, n = 8) show no significant changes from the basal values (Pre). Data points shown are means. * $p < 0.01$ compared with the high fat diet with ethanol group.

Statistical analyses. Results are expressed as means±standard deviation. Student's t test for the comparison of two independent means was used to test for the significance of the difference between the means of two groups. The relationship between normally distributed variables was assessed using Pearson's coefficient of correlation. All tests were two-tailed. Because of the multiple comparisons performed between groups of animals, a conservative significance level of 0.01 was used.

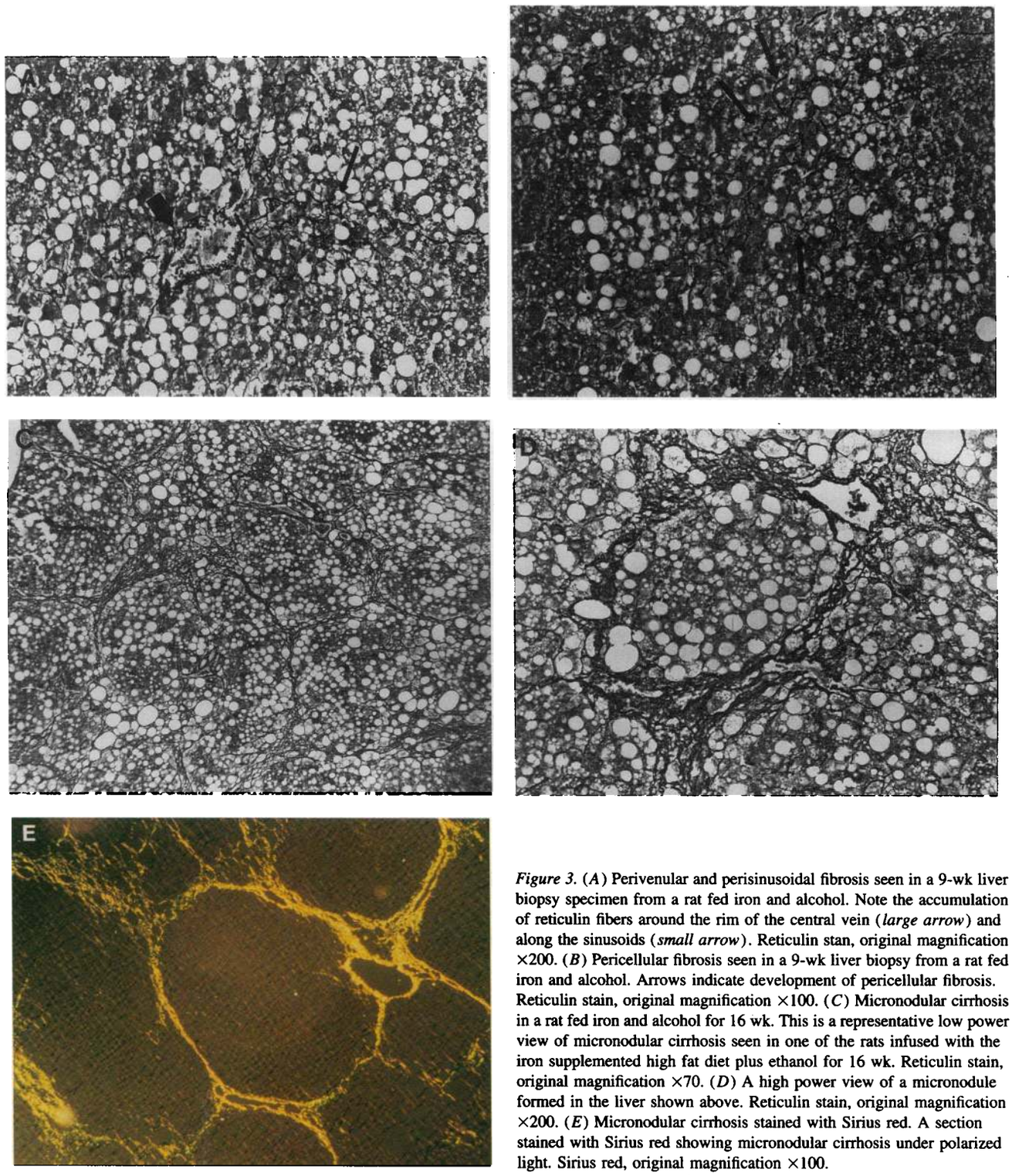

Figure 3. (*A*) Perivenular and perisinusoidal fibrosis seen in a 9-wk liver biopsy specimen from a rat fed iron and alcohol. Note the accumulation of reticulin fibers around the rim of the central vein (*large arrow*) and along the sinusoids (*small arrow*). Reticulin stan, original magnification ×200. (*B*) Pericellular fibrosis seen in a 9-wk liver biopsy from a rat fed iron and alcohol. Arrows indicate development of pericellular fibrosis. Reticulin stain, original magnification ×100. (*C*) Micronodular cirrhosis in a rat fed iron and alcohol for 16 wk. This is a representative low power view of micronodular cirrhosis seen in one of the rats infused with the iron supplemented high fat diet plus ethanol for 16 wk. Reticulin stain, original magnification ×70. (*D*) A high power view of a micronodule formed in the liver shown above. Reticulin stain, original magnification ×200. (*E*) Micronodular cirrhosis stained with Sirius red. A section stained with Sirius red showing micronodular cirrhosis under polarized light. Sirius red, original magnification ×100.

Results

Weight gain, liver weight, ratio of liver weight to body weight, and blood alcohol concentration. Differences in weight gain among the four groups of animals were not statistically significant (Table I). By contrast, liver weights of both groups of alcohol-fed rats (high fat diet with ethanol; and high fat diet with iron and ethanol) were markedly increased by about two-fold when compared with the corresponding control group. As a consequence, if the comparisons were made with respect to weight gain excluded the increase in liver weight, both alcohol-fed groups gained significantly less body weight than the corre-

Table I. Body Weight Gain, Liver Weight, Ratio of Liver Weight to Body Weight and Blood Alcohol Levels of Animals Fed Control or Ethanol Diet with or without Iron Supplementation for 16 wk

	Weight gain	Liver weight	Ratio of liver weight to body weight	Blood alcohol
	g	*g*		*mg/dL*
High-fat diet (n = 8)	228.6±42.2	17.3±0.6	0.028±0.002	—
High-fat diet with iron (n = 9)	191.5±35.4	16.7±1.4	0.029±0.002	—
High-fat diet with ethanol (n = 7)	208.2±40.0	30.2±2.0*	0.050±0.003*	307±28
High-fat diet with iron and ethanol (n = 10)	175.9±34.6	33.7±4.6*‡	0.058±0.008*‡	350±70

These data were collected after 16 wk of intragastic infusion of a high-fat diet with ethanol or isocaloric glucose with or without supplementation with carbonyl iron. Data are shown as means±standard deviation. * $P < 0.0001$ compared with group receiving high-fat diet. ‡ $P < 0.0001$ compared with group receiving high-fat diet with iron.

sponding control groups and the iron-supplemented, alcohol-fed group gained significantly less body weight than the high fat diet with ethanol group (data not shown). If comparisons were made with respect to the final ratio of liver weight to body weight, the ratios were significantly higher in both ethanol-fed groups when compared to the corresponding control group. Mean blood alcohol concentrations in the two groups fed ethanol were similar (Table I).

Plasma and liver non-heme iron concentration. Plasma and liver non-heme iron concentrations at 9 and 16 wk are shown in Table II. The concentrations in plasma and liver at 16 wk were or tended to be higher than those at 9 wk in all groups, demonstrating an age-dependent increase as previously reported (34). Ethanol feeding alone (high fat diet with ethanol) did not affect plasma and liver non-heme iron concentrations. Iron supplementation caused a two to threefold increase in both plasma and liver non-heme iron in alcohol-fed and control-pair fed animals (high fat diet with iron; and high fat diet with iron and ethanol). Hepatic non-heme iron concentrations in ethanol-fed groups with or without iron supplementation were significantly lower than those in respective control groups. This reduction is most likely to be due to a twofold increase in liver weights in both ethanol-fed groups as compared with the control groups (Table I).

Liver lipid peroxidation. As shown in Fig. 1 and as predicted from a previous study (8), animals-fed high fat diet with ethanol had increased hepatic levels of MDA (Fig. 1 *A*) and 4HNE (Fig. 1 *B*) compared with the pair-fed, high fat diet group. These changes were accompanied by a significant depression in the GSH level (Fig. 1 *C*), indicating enhanced oxidant stress in the ethanol-fed animals. Iron supplementation caused further increases in the MDA and 4HNE levels in the ethanol-fed rats (high fat diet with iron and ethanol) resulting in concentrations twofold higher than those of the group receiving high fat diet with ethanol. The GSH concentrations in the ethanol-fed group with or without iron were reduced to a similar extent. MDA, 4HNE and GSH concentrations in the high fat diet with iron group were not significantly different from those in the high fat diet group.

Plasma aminotransferase concentrations. The ALT and AST concentrations are depicted in Fig. 2, *A* and *B*, respectively. At 9 wk, plasma levels of both enzymes were elevated two- to threefold by ethanol feeding alone (high fat diet with ethanol) compared to the high fat diet group. Iron supplementation resulted in an additional two- to threefold increase in the concentrations of these enzymes (high fat diet with iron and ethanol). At 16 wk, the ALT level in this group continued to be twofold higher than that of the high fat diet with ethanol group while the AST levels were not significantly different.

Liver histopathology. After 9 wk, enhanced alcoholic liver fibrogenesis with iron supplementation was already evident in liver biopsy specimens. Diffuse perivenular (Fig. 3 *A*), perisi-

Table II. Plasma and Liver Non-heme Iron Concentrations after 9 and 16 wk of Feeding the Diets Shown

	9 wk		16 wk	
	Plasma iron	Liver non-heme iron	Plasma iron	Liver non-heme iron
	μg/dL	*μg/g, wet wt*	*μg/dL*	*μg/g, wet wt*
High-fat diet (n = 7)	83.3±11.8	140.3±10.4	167.0±14.7‖	241.0±17.7‖
High-fat diet with iron (n = 8)	158.7±5.5*	400.0±46.5*	231.7±41.0*‖	627.7±130.5*‖
High-fat diet with ethanol (n = 5)	80.7±4.7‡	142.3±8.2‡	210.0±30.5‖	191.5±2.5*‡‖
High-fat diet with iron and ethanol (n = 9)	194.8±25.7*‡§	359.7±50.5*§	326.5±45.7*‡§‖	406.7±75.8*‡§

Blood and liver biopsy specimens were collected for determination of plasma and liver non-heme iron concentrations, respectively, after 9 wk of feeding the diets shown. These determinations were repeated on specimens obtained at autopsy at 16 wk. Because of technical difficulties and sample size limitations, iron measurements could not be done in some animals in each of the experimental groups. Data are shown as means ± standard deviation. * $P < 0.005$ compared with group receiving high-fat diet. ‡ $P < 0.005$ compared with group receiving high-fat diet with iron. § $P < 0.0005$ compared with group receiving high-fat diet with ethanol. ‖ $P < 0.005$ compared with group at 9 wk.

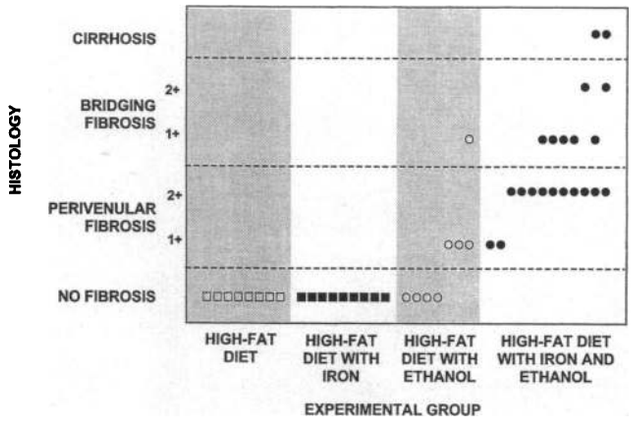

Figure 4. Summary of histological grading of liver fibrosis in the four dietary groups. Liver fibrosis was evaluated and graded as described in Methods. Changes in each animal are depicted in a vertical manner for each of histological criteria (1+: focal; and 2+: diffuse). Note apparent potentiation by iron supplementation of alcohol-induced liver fibrosis.

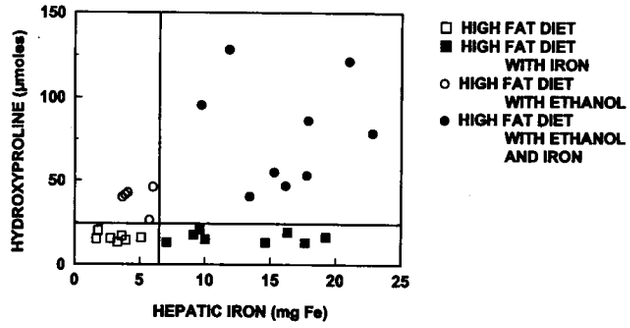

Figure 5. Total hepatic hydroxyproline and iron content. The total hepatic hydroxyproline content in the four groups of animals were depicted as a function of the total hepatic iron content, both determined at 16th wk. Note higher hydroxyproline content in animals given ethanol and iron as compared to that in other three groups.

nusoidal (Fig. 3 *A*) and pericellular (Fig. 3 *B*) fibrosis were present in most of the animals fed high fat diet with iron and ethanol while such changes were not evident or restricted to focal areas in animals fed high fat diet with ethanol (data not shown). Results on induction of liver fibrosis at the 16 wk are summarized in Fig. 4. Neither animals fed high fat diet nor those fed high fat diet with iron showed liver fibrosis even though focal necrosis and inflammation were noted in some of the rats given high fat diet with iron. Feeding high fat diet with ethanol for 16 wk caused moderate to severe fatty liver in all, focal centrilobular necrosis and inflammation in 43% of the animals (data not shown) with focal perivenular and bridging fibrosis in 29% (Fig. 4). These focal and mild fibrotic changes are typical for this model under the high fat diet and alcohol regimen. By contrast, the group which receive high fat diet with iron and ethanol showed marked potentiation of liver fibrogenesis evidenced by diffuse lesions in the majority of the animals (Fig. 4). This diffuse development of perivenular and bridging fibrosis (predominantly central-central) appeared to reflect exacerbation of the pattern of fibrotic changes seen in the high fat diet with ethanol group. In addition, two animals in the given high fat diet with iron and ethanol developed micronodular cirrhosis (Fig. 3, *C*–3*E*).

Hepatic hydroxyproline level. Chemical assessment of hepatic collagen content by measurement of hydroxyproline confirmed the histological observation of enhanced alcoholic liver fibrogenesis in the high fat diet with iron and ethanol group (Fig. 5). Both the hydroxyproline concentration expressed per gram of liver wet weight (2.56±0.58 μmoles/gram) and the total content of this amino acid in the whole liver (89.60±9.92 μmoles: individual data shown in Fig. 5) were significantly increased by twofold as compared to those in the animals given high fat diet with ethanol (1.32±0.32 μmoles/g liver and 42.24±6.95 μmoles/liver) and by more than twofold when compared with the high fat diet with iron group (0.99±0.18 μmoles/gram and 17.83±1.56 μmoles/liver).

MDA- and 4HNE-derived protein adducts in the liver. Immunostaining using antibodies specific for the MDA- (Fig. 6) and 4HNE- (Fig. 7) derived protein epitopes revealed distinct positive reactions in all ethanol-fed animals. The MDA-derived proteins were also present at the same sites as the HNE-derived adducts, although the intensity of the reaction for the MDA-derived epitopes was usually stronger. In the group fed high fat diet with ethanol, positive reactions for the aldehyde-derived epitopes were restricted to the perivenular zone (Figs. 6 *B* and 7 *B*), while in the animals given high fat diet with iron and ethanol, more intense, positive reactions were found to occur through all zones in a diffuse manner (Figs. 6 *A* and 7 *A*). No immunoreactivities were found for both MDA and 4HNE adducts in the high fat diet group (Figs. 6 *C* and 7 *C*). Slight staining was focally found in some of the animals fed high fat diet with iron while others showed no immunostaining (data not shown). No specific staining was observed when livers from animals that received ethanol, with or without iron, were stained with non-immune serum (Fig. 8 *A* and *B*).

Collagen and TGFβ1 mRNA expression. Northern blot analyses of liver RNA samples showed a pattern of changes similar to that seen in the chemical and histological studies, demonstrating iron-induced potentiation of alcoholic liver fibrogenesis as indicated by increased steady-state mRNA levels for procollagen α1(I) and TGFβ1 in the animals fed high fat diet with iron and ethanol as compared with other three groups; a representative blot is shown in Fig. 9 where a RNA sample from a rat with liver cirrhosis induced by high fat diet with iron and ethanol (HFD + Iron + Ethanol) showed markedly elevated levels of procollagen α1(I) mRNA while a rat fed high fat diet with ethanol (HFD + Ethanol) had a mild increase. For quantitative assessment of procollagen α1(I) and TGFβ1 mRNA, Northern blots of samples from the different dietary groups (4–5 samples per group) were densitometrically analyzed, standardized with β-actin values, and compared to results from high fat diet animals which were arbitrarily set at 1.0. The relative changes derived from this analysis for procollagen α1(I) and TGFβ1 mRNA in the different dietary groups were: 4.7±2.6 ($P < 0.01$) and 1.7±0.6 ($P = 0.06$) for the high fat diet with ethanol group; 1.5±0.7 and 1.7±0.8 (both $P > 0.05$) for the high fat diet with iron group; and 16.7±8.5 ($P < 0.001$) and 2.8±1.0 ($P < 0.01$) for the high fat diet with iron and ethanol group, respectively.

To examine the cellular basis for the enhanced collagen and TGFβ1 mRNA expression in the livers of the animals fed high fat diet with iron and ethanol, we analyzed the procollagen

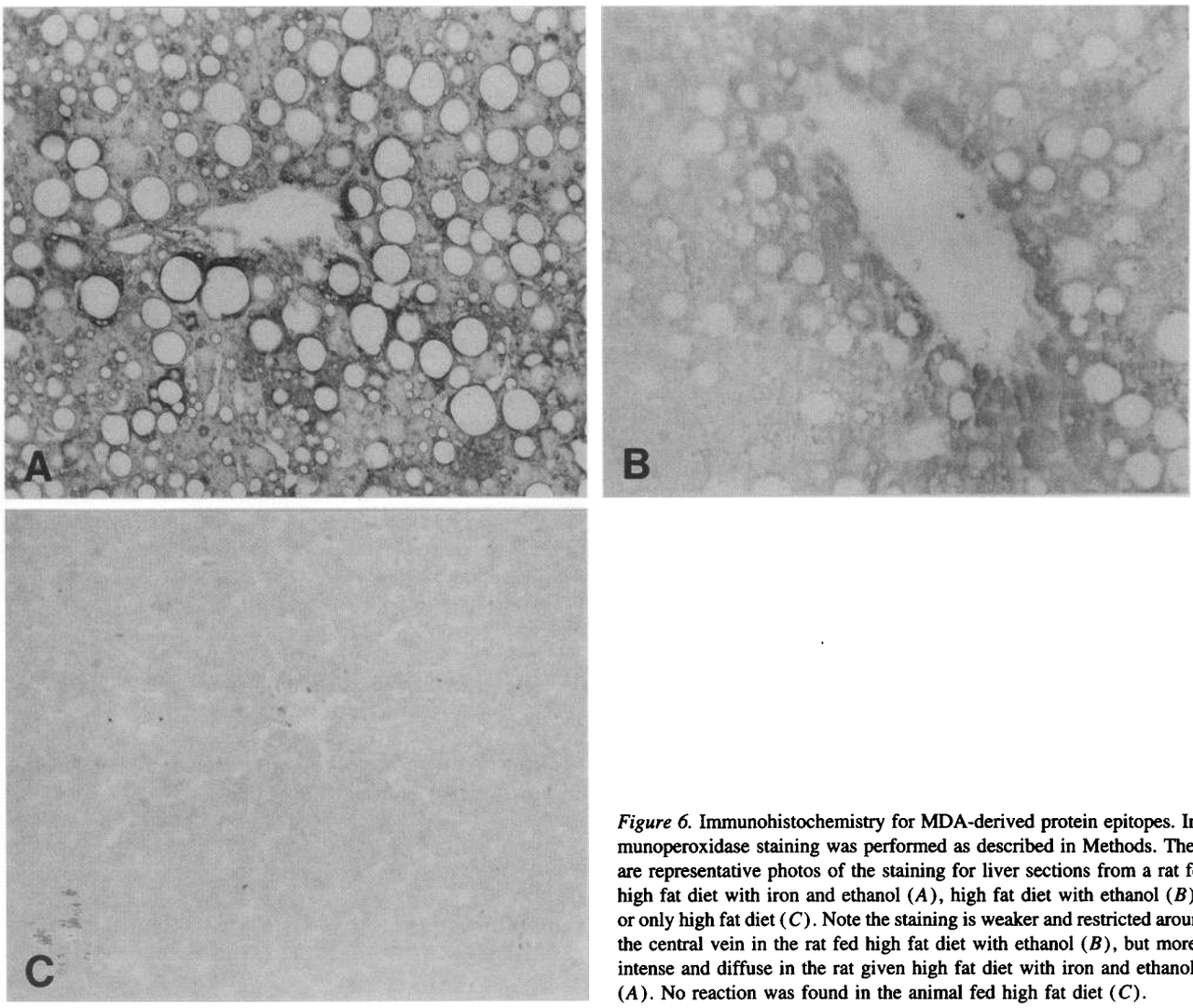

Figure 6. Immunohistochemistry for MDA-derived protein epitopes. Immunoperoxidase staining was performed as described in Methods. These are representative photos of the staining for liver sections from a rat fed high fat diet with iron and ethanol (*A*), high fat diet with ethanol (*B*), or only high fat diet (*C*). Note the staining is weaker and restricted around the central vein in the rat fed high fat diet with ethanol (*B*), but more intense and diffuse in the rat given high fat diet with iron and ethanol (*A*). No reaction was found in the animal fed high fat diet (*C*).

α1(I) and TGFβ1 mRNA levels in freshly isolated hepatic stellate cells, the perisinusoidal cells believed to be responsible for production of excessive extracellular matrices in liver fibrosis. As shown in a representative Northern blot (Fig. 10), accentuated increases in procollagen α1(I) and TGFβ1 mRNA levels were observed in the animals fed high fat diet with iron and ethanol (HFD + Iron + Ethanol), which paralleled the changes seen in the Northern blot analysis of the liver RNA samples. The relative increases in mRNA expression by hepatic stellate cells in this group (with normalization to β-actin and comparison to the high fat diet group) were 29.5±9.1 for procollagen α1(I) and 8.3±2.4 for TGFβ1 (both $n = 4$, $P < 0.01$). These results established that the iron-induced potentiation of alcoholic liver fibrosis was closely associated with fibrogenic activation of hepatic stellate cells.

Correlation of liver collagen content with 4HNE and iron. The relationship between the hepatic concentration of 4-HNE and the liver content of hydroxyproline was examined in the group fed high fat diet with iron and ethanol using a correlation analysis (Fig. 11). The analysis revealed a positive, significant correlation between these parameters. Interestingly, no significant correlation was found between the hydroxyproline content and the non-heme iron content in the livers of this group (data not shown). When the same analysis was performed with the animals from both groups given high fat diet with ethanol and high fat diet with iron and ethanol, it showed a tendency for the correlation ($r = 0.52$, $P = 0.086$), but did not achieve statistical significance.

Discussion

The experimental results reported here provide support for the hypothesis that the livers of ethanol-fed rats are more susceptible to iron-catalyzed lipid peroxidation which, in turn, potentiates hepatic fibrogenesis. In ethanol-fed animals, accentuated liver injury and fibrogenesis were induced by slightly elevated liver iron concentrations, which were still within or near the upper limit of the normal range in human subjects ($\sim$ 681 μg iron per gram of liver, wet weight) (20). Even though this range of non-heme iron concentrations produced no or minimal histological or biochemical abnormalities in pair-fed control rats given iron but no alcohol, it caused marked potentiation of

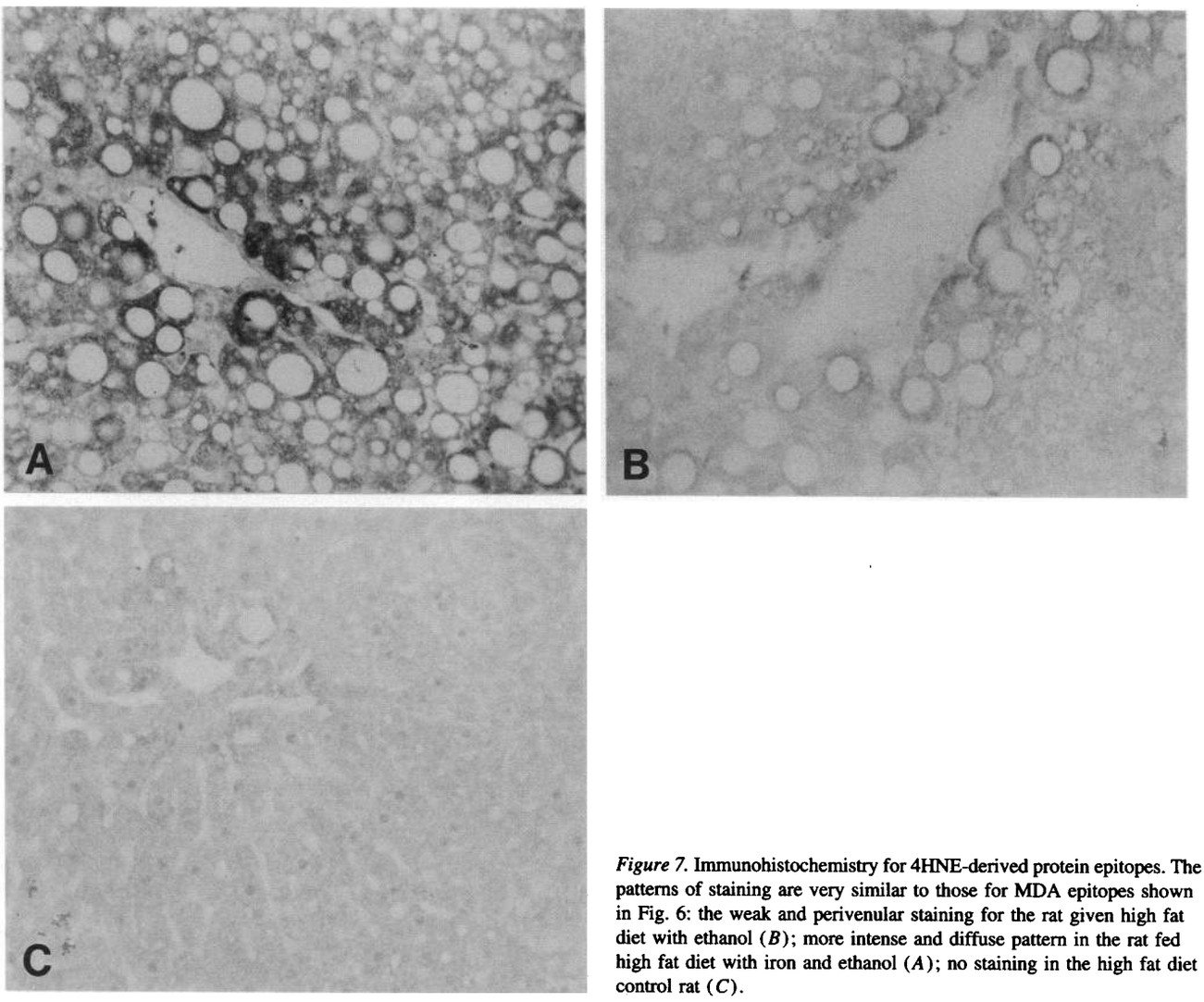

Figure 7. Immunohistochemistry for 4HNE-derived protein epitopes. The patterns of staining are very similar to those for MDA epitopes shown in Fig. 6: the weak and perivenular staining for the rat given high fat diet with ethanol (*B*); more intense and diffuse pattern in the rat fed high fat diet with iron and ethanol (*A*); no staining in the high fat diet control rat (*C*).

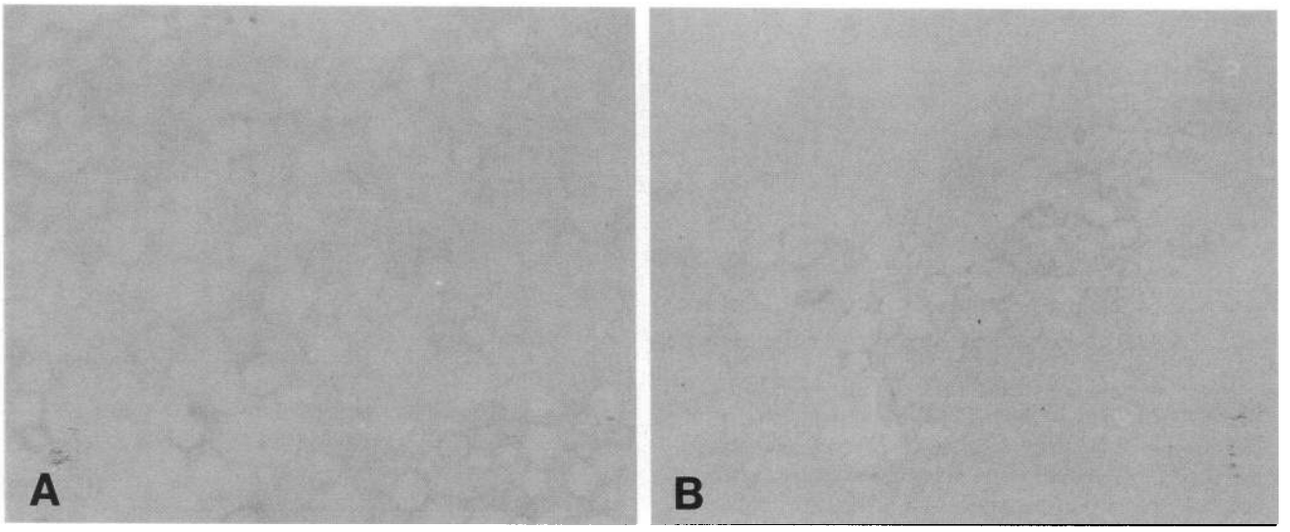

Figure 8. Immunohistochemistry with non-immune serum. No specific staining was detected when the liver from the rat given high fat diet with iron and ethanol (*A*) or high fat diet with ethanol (*B*) was stained with non-immune serum.

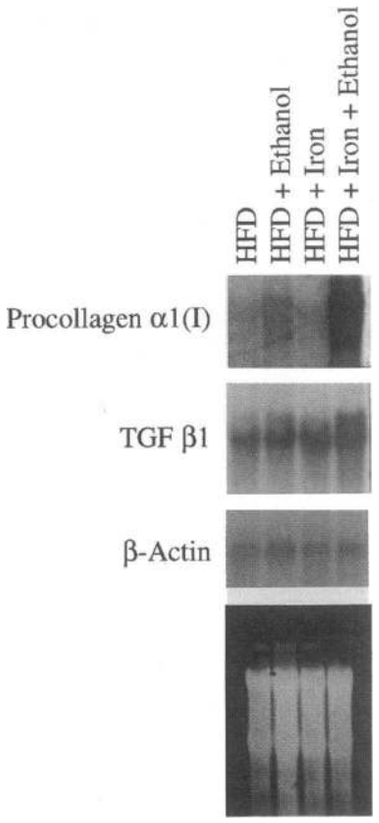

Figure 9. Northern blot analyses of total liver RNA for collagen and TGFβ1 mRNA expression. Twenty micrograms of total liver RNA samples from the rat fed: high fat diet (*HFD*); high fat diet with ethanol (*HFD + Ethanol*); high fat diet with iron (*HFD + Iron*); or high fat diet with iron and ethanol (*HFD + Iron + Ethanol*), were subjected to Northern blot analysis using ^{32}P-labeled procollagen α1(I) and TGFβ1 cDNAs. Note marked increases in procollagen mRNA levels in the rat given high fat diet with iron and ethanol which developed micronodular liver cirrhosis while a mild increase in this mRNA can be seen in the rat fed high fat diet with ethanol. The increased TGFβ1 mRNA expression can also be observed in the HFD + Iron + Ethanol.

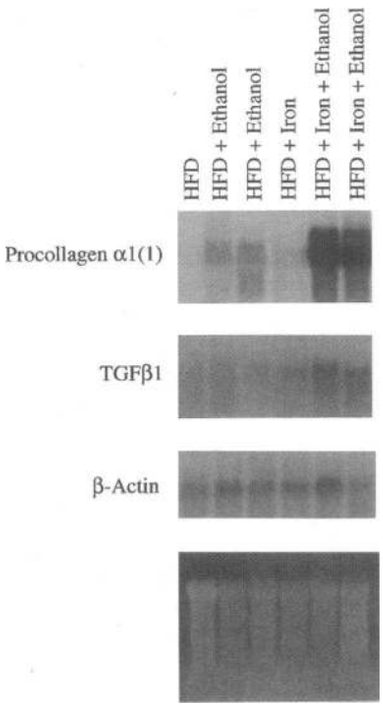

Figure 10. Northern blot analyses of hepatic stellate cell RNA for collagen and TGFβ1 mRNA expression. 20 μg of hepatic stellate cell RNA samples were subjected to Northern blot analysis as described in Methods. Note prominent increases in procollagen α1(I) and TGFβ1 mRNA levels in the animals fed high fat diet with iron and ethanol (HFD + Iron + Ethanol), both of which developed micronodular liver cirrhosis.

experimental alcoholic liver disease. This result obviously has a clinical implication that the threshold concentration of hepatic iron for developing liver damage in patients with alcoholic liver disease may actually be lower than normal subjects due to the ethanol-induced sensitization. Increased concentrations of stainable or chemically measured hepatic iron are sometimes seen in association with alcoholic liver disease (35, 36), and may reach the levels 2–3 times higher than those in normal subjects or those seen in the iron-supplemented animals in the present study. Thus a combination of the elevated hepatic iron concentrations and the increased sensitivity to iron-catalyzed oxidant stress may result in exacerbated oxidant stress contributing to the pathogenesis and progression of alcoholic liver disease.

Our previous studies have suggested two potential sources for the increased sensitivity to iron-catalyzed oxidant stress in animals fed ethanol. First, chronic excessive ethanol consumption markedly induces CYP2E1, causing a several fold increase in the content of this cytochrome and a 20-fold enhancement of its catalytic activity in hepatic microsomes (4). This finding has now been confirmed by other investigators (3, 15, 16, 17). This induction accounted for the enhanced sensitivity of the microsomes to iron-catalyzed lipid peroxidation in vitro (4), and may possibly be responsible for the enhanced oxidant injury in the iron and ethanol fed rats in the present study. Second,

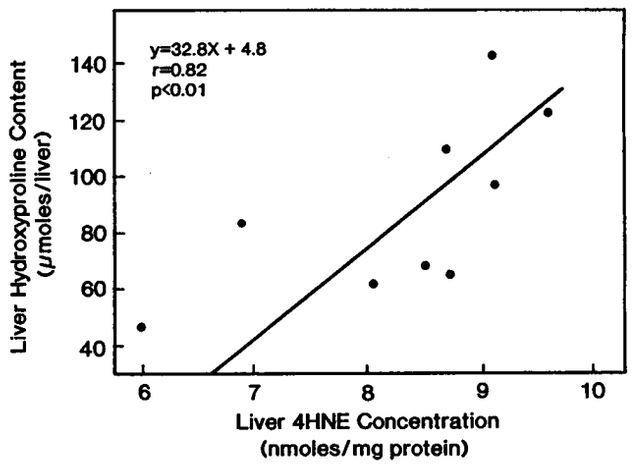

Figure 11. Correlation between liver 4HNE concentration and collagen accumulation. Relationship between the 4HNE concentration and the hydroxyproline content in the livers of rats fed high fat diet with iron and ethanol for 16 wk, was evaluated by a correlation analysis. Note a significant, positive correlation between the two parameters.

mitochondria may also be a site of the oxidant stress because enhanced lipid peroxidation has also been documented to occur in this organelle in both ethanol-fed (8) and iron-overloaded (37) animals. Moreover, this organelle exhibits a specific defect of glutathione depletion during the development of experimental alcoholic liver injury (7).

Another hypothesis supported by the results from the present study is the pathogenetic role of lipid peroxidation and its aldehydic products in liver fibrogenesis. This hypothesis was originally proposed when MDA (18), acetaldehyde (1), and the basal lipid peroxidation (38) were shown to stimulate collagen gene expression in cultured fibroblasts. These observations in vitro were recently extended to the cultures of hepatic stellate cells, which are critically involved in liver fibrogenesis (11). Studies have now demonstrated that collagen gene expression is stimulated by 4HNE, another major aldehydic lipid-peroxidation product (19). In the present study, the increases in both MDA and 4HNE levels in the livers of iron and alcohol-fed animals were associated with a marked enhancement of liver fibrogenesis. Furthermore, a positive correlation was found between hepatic 4HNE concentration, immunohistochemical localization of MDA- and 4HNE-derived epitopes, and collagen accumulation in these animals. Along with the direct evidence for stimulation of collagen gene expression by 4HNE and MDA, these results provide strong evidence for a possible mechanistic role of lipid peroxidation and its products in liver fibrosis.

Alternatively, oxidant stress may stimulate hepatic fibrogenesis in a manner independent from lipid peroxidation. For example, oxidant stress can induce intracellular signaling as recently shown in a variety of cells (39–42) which may involve activation of phospholipase A_2 (39), an increase in cytosolic calcium concentration (40), and induction of nuclear factors (41, 42). Therefore, these intracellular mechanisms may directly or indirectly contribute to the effects of iron-catalyzed oxidant stress on collagen gene expression. Further studies are obviously needed to elucidate cellular and molecular mechanisms which underlie iron-potentiated alcoholic liver fibrogenesis.

Acknowledgments

We thank Professor Hermann Esterbauer of the University of Graz for his generous gift of authentic 4HNE. We also thank Zhen-Zhen Luo, Sandy Yeager, Chong W. Kim, H. Ying Chen, Timothy Highman, and Vanessa Bednarik for their valuable technical assistance.

This study was supported by U.S. Public Health Service grants AA00603 and HL0714, and the Department of Veterans Affairs.

References

1. Brenner, D. A., and M. Chojkier. 1987. Acetaldehyde increases collagen gene transcription in cultured human fibroblasts. *J. Biol. Chem.* 262:17690–17695.

2. Casini, A., M. Cunningham, M. Rojkind, and C. S. Lieber. 1991. Acetaldehyde increases procollagen type I and fibronectin gene transcription in cultured rat fat-storing cells through a protein synthesis-dependent mechanism. *Hepatology.* 13:758–765.

3. French, S. W., K. Wong, L. Jui, E. Albano, A.-L. Hagbjörk, and M. Ingelman-Sundberg. 1993. Effect of ethanol on cytochrome P450 (CYP2E1), lipid peroxidation and serum protein adduct formation in relation to liver pathology pathogenesis. *Exp. Mol. Pathol.* 58:61–75.

4. Castillo, T., D. R. Koop, S. Kamimura, G. Triadafilopoulos, and H. Tsukamoto. 1992. Role of cytochrome P4502E1 in ethanol-carbon tetrachloride- and iron-dependent microsomal lipid peroxidation. *Hepatology.* 16:992–996.

5. Reinke, L. A., Y. Kotake, P. B. McCay, and E. G. Janzen. 1991. Spin-trapping studies of hepatic free radicals formed following the acute administration of ethanol to rats: in vivo detection of 1-hydroxyethyl radicals with PBN. *Free Radical Biol. & Med.* 11:31–39.

6. Knecht, K. T., R. G. Thurman, and R. P. Mason. 1993. Role of superoxide and trace transition metals in the production of α-hydroxyethyl radical from ethanol by microsomes from alcohol dehydrogenase-deficient deer mice. *Arch. Biochem. Biophys.* 303:339–348.

7. Hirano, T., N. Kaplowitz, H. Tsukamoto, S. Kamimura, and J. C. Fernandez-Checa. 1992. Hepatic mitochondrial glutathione depletion and progression of experimental alcoholic liver disease in rats. *Hepatology.* 16:1423–1427.

8. Kamimura, S., K. Gaal, R. S. Britton, B. R. Bacon, G. Triadafilopoulos, and H. Tsukamoto. 1992. Increased 4-hydroxynonenal levels in experimental alcoholic liver disease: association of lipid peroxidation with liver fibrogenesis. *Hepatology.* 16:448–453.

9. Matsuoka, M., and H. Tsukamoto. 1990. Stimulation of hepatic lipocyte collagen production by Kupffer cell-derived transforming growth factor β: implication for a pathogenetic role in alcoholic liver fibrogenesis. *Hepatology.* 11:599–605.

10. Friedman, D. L. 1993. The cellular basis of hepatic fibrosis: mechanisms and treatment strategies. *N. Engl. J. Med.* 328:1828–1835.

11. Tsukamoto, H., S. J. Towner, L. M. Ciofalo, and S. W. French. 1986. Ethanol-induced liver fibrosis in rats fed high fat diet. *Hepatology.* 6:814–822.

12. Tsukamoto, H., K. Gaal, and S. W. French. 1990. Insights into the pathogenesis of alcoholic liver necrosis and fibrosis; status report. *Hepatology.* 12:599–608.

13. Tsukamoto H., 1993. Oxidative stress, antioxidants, and alcoholic liver fibrogenesis. *Alcohol.* 10:465–467.

14. Yoo J-S, H., S. M. Ning, C. B. Pantuck, E. J. Pantuck, and C. S. Yang. 1991. Regulation of hepatic microsomal cytochrome P450IIE1 level by dietary lipids and carbohydrates in rats. *J. Nutr.* 121:959–965.

15. Takahashi, H., I. Johansson, S. W. French, and M. Ingelman-Sundberg. 1992. Effects of dietary fat composition on activities of the microsomal ethanol oxidizing system and ethanol-inducible cytochrome P450 (CYP2E1) in the liver of rats chronically fed ethanol. *Pharmacol. Toxicol.* 70:347–352.

16. Nanji, A. A., S. Zhao, R. G. Lamb, A. J. Dannenberg, S. M. H. Sadrzadeh, and D. J. Waxman. 1994. Changes in cytochromes P-450, 2E1, 2B1, and 4A, and phospholipase A and C in the intragastric feeding rat model for alcoholic liver disease: relationship to dietary fats and pathologic liver injury. *Alcoholism Clin. Exp. Res.* 18:902–908.

17. Morimoto, M., A.-L. Hagbjörk, A. A. Nanji, M. Ingelman-Sundberg, K. O. Lindros, P. C. Fu, E. Albano, and S. W. French. 1993. Role of cytochrome P4502E1 in alcoholic liver disease pathogenesis. *Alcohol.* 10:459–464.

18. Chojkier, M., K. Houglum, J. Solis-Herruzo, and D. A. Brenner. 1989. Stimulation of collagen gene expression by ascorbic acid in cultured human fibroblast. A role for lipid peroxidation? *J. Biol. Chem.* 264:16957–16962.

19. Parola, M., M. Pinzani, A. Casini, E. Albano, G. Po li, A. Gentilini, P. Gentilini, and M. W. Dianzani. 1993. Stimulation of lipid peroxidation or 4-hydroxynonenal treatment increases procollagen a1 (I) gene expression in human liver fat-storing cells. *Biochem. Biophy. Res. Commun.* 194:1044–1050.

20. Weinfeld, A. 1964. Storage iron in man. *Acta Med. Scand. (Suppl.)* 427:1–155.

21. Torrance, J. D., and T. H. Bothwell. 1980. Tissue iron stores. *In* Iron. J. Cook, editor. Churchill-Livingstone/New York. 90–115.

22. Uchiyama, M., M. Mihara. 1978. Determination of malonaldehyde precursor in tissues by thiobarbituric acid test. *Anal. Biochem.* 86:271–278.

23. Esterbauer, H., K. H. Cheeseman, M. U. Dianzani, G. Poli, and T. F. Slater. 1982. Separation and characterization of the aldehydic products of lipid peroxidation stimulated by ADP-Fe^{2+} in rat liver microsomes. *Biochem. J.* 208:129–140.

24. Benedetti, A., A. Pompella, R. Fulceri, A. Romani, and M. Comporti. 1986. Detection of 4-hydroxynonenal and other lipid peroxidation products in the liver of bromobenzene-poisoned mice. *Biochem. Biophys. Acta.* 876:658–666.

25. Griffith, O. W. 1980. Determination of glutathione and glutathione disulfide using glutathione reductase and 2-vinylpyridine. *Anal. Biochem.* 106:207–212.

26. Allen K. G. D., and J. R. Arthur. 1987. Inhibition by 5-sulfosalicylic acid of the glutathione reductase recycling assay for glutathione analysis. *Clin. Chem. Acta.* 162:237–239.

27. Jamall, I. S., V. N. Finelli, and S. S. Que Hee. 1981. A simple method to determine nanogram levels of 4-hydroxyproline in biological tissues. *Anal. Biochem.* 112:70–75.

28. Niemelä, O., S. Parkkila, S. Ylä-Herttuala, C. Halstead, J. Witztum, A. Lanca, and Y. Israel. 1994. Covalent protein adducts in the liver as a result of ethanol metabolism and lipid peroxidation. *Lab. Invest.* 20:537–546.

29. Palinski, W., S. Yla-Herttuala, M. E. Rosenfeld, S. W. Butler, S. A. Socher, S. Parthasanthy, L. K. Cuttiss, and J. L. Witzhum. 1990. Antisera and

monoclonal antibodies specific for epitopes generated during oxidative modification of low density lipoprotein. *Arteriosclerosis.* 10:325–335.

30. Esterbauer, H., G. Frirgens, O. Quehenberger, and E. Keller. 1987. Autooxidation of human low density lipoprotein: loss of polyunsaturated fatty acids and vitamin E and generation of aldehyde. *J. Lipid Res.* 28:495–509.

31. Chomczynski, P. L., and N. Sacchi. 1987. Single-step method of RNA isolation by acid guanidium thiocyanate-phenol-chloroform extraction. *Anal. Biochem.* 162:156–159.

32. Genovese, C., D. Rowe, and B. Kream. 1984. Construction of DNA sequences complementary to rat alpha 1 and alpha 2 collagen mRNA and their use in studying the regulation of Type I collagen synthesis by 1.25-dihydroxyvitamin D. *Biochemistry.* 23:6210–6216.

33. Derynck, R., J. A. Jarrette, E. Y. Chen, D. H. Eaton, J. R. Bell, R. K. Assoian, A. B. Roberts, M. B. Sporn, and D. V. Goeddel. 1983. Human transforming growth factor-β complementary DNA sequence and expression in normal and transformed cells. *Science (Wash. DC).* 316:701–705.

34. Park, C. H., B. R. Bacon, G. M. Brittenham, and A. S. Tavill. 1987. Pathology of dietary carbonyl iron overload in rats. *Lab. Invest.* 57:555–563.

35. Bell, E. T. 1955. Relation of portal cirrhosis to haemochromatosis and to diabetes mellitus. *Diabetes.* 4:435–446.

36. Bassett, M. L., J. W. Holliday, and L. W. Powell. 1986. Value of hepatic iron measurements in early hemochromatosis and determination of the critical iron level associated with fibrosis. *Hepatology.* 6:24–29.

37. Bacon, B. R., A. S. Tavill, G. M. Brittenham, C. H. Park, and R. O. Recknagel. 1983. Hepatic lipid peroxidation in vivo in rats with chronic iron overload. *J. Clin. Invest.* 71:429–439.

38. Houglum, K., D. A. Brenner, and M. Chojkier. 1991. d-a-Tocopherol inhibits collagen a_1(I) gene expression in cultured human fibroblasts. Modulation of constitutive collagen gene expression by lipid peroxidation. *J. Clin. Invest.* 87:2230–2235.

39. Zhang J. R., and A. Sevanian. 1993. The genotoxic effects of arachidonic acid in V79 cells are mediated by peroxidation products. *Toxicol. & Appl. Pharmacol.* 121:193–202.

40. Livingston, F. R., E. M. Lui, G. A. Loeb, H. J. Forman. 1992. Sublethal oxidant stress induces a reversible increase in intracellular calcium dependent on NAD(P)H oxidation in rat alveolar macrophages. *Arch. of Biochem. & Biophy.* 299:83–91.

41. DeForge, L. E., A. M. Preston, E. Takenchi, J. Kenny, L. A. Boxers, and D. G. Remick. 1993. Regulation of interleukin 8 gene expression by oxidative stress. *J. Biol. Chem.* 268:25568–25576.

42. Baeuerle, P. A., and D. Baltimore. 1988. IkB:A Specific Inhibitor of the NF-kB Transcription Factor. *Science (Wash. DC).* 242:540–546.